Some fundamental (and often overlooked) considerations underlying the free ion activity and biotic ligand models

Hassler, Christel; Slaveykova, Vera; Wilkinson, Kevin J

SETAC PRESS

Environmental Toxicology and Chemistry, Vol. 23, No. 2, pp. 283–291, 2004

Printed in the USA
0730-7268/04 $12.00 + .00

SOME FUNDAMENTAL (AND OFTEN OVERLOOKED) CONSIDERATIONS UNDERLYING THE FREE ION ACTIVITY AND BIOTIC LIGAND MODELS

CHRISTEL S. HASSLER, VERA I. SLAVEYKOVA, and KEVIN J. WILKINSON*
Analytical and Biophysical Environmental Chemistry (CABE), University of Geneva, Sciences II, 30 Quai Ernest-Ansermet, 1211 Geneva 4, Switzerland

(*Received* 13 *March* 2003; *Accepted* 25 *June* 2003)

Abstract—Trace metal bioavailability is often evaluated on the basis of steady-state models such as the free ion activity model (FIAM) and the biotic ligand model (BLM). Some of the assumptions underlying these models were verified by examining Pb and Zn uptake by the green microalga *Chlorella kesslerii*. Transporter bound metal ($\{M\text{-}R_{cell}\}$) and free ion concentrations ($[M^{Z+}]$) were related to experimentally determined uptake fluxes (J_{int}). Although the BLM and FIAM correctly predicted Pb uptake in the absence of competing ions, they failed to predict competitive interactions with Ca^{2+}, likely because of modifications of the algal surface charge and the active nature of Ca^{2+} transport. Zinc transport is also active; in this case, both the internalization rate constant (k_{int}) and the equilibrium constant for the binding of Zn to the transport sites ($K_{Zn\text{-}R_{cell}}$) varied as a function of $[Zn^{2+}]$ in the bulk solution. For this reason, Zn uptake could not be modeled by the steady-state models either in the presence or absence of competitors (Cd and Ca). Furthermore, the role of Cu on Pb and Zn adsorption and uptake could not be predicted by either model because of secondary effects on the algal physiology and membrane permeability. Finally, a 17°C reduction in temperature resulted in a two- to fivefold decrease in membrane permeability of the metals, an observation that also is unaccounted for by either the FIAM or BLM. This paper emphasizes the limitations of the models in well-controlled laboratory systems with the goal of extrapolating the results to complex environmental systems.

Keywords—Free ion activity model Biotic ligand model Uptake Trace metal Competition

INTRODUCTION

It is currently well accepted that in order to predict trace metal effects on aquatic organisms, it is necessary to take chemical speciation into account rather than to simply measure total metal concentrations. Nonetheless, a fundamental understanding of the relationship between trace metal speciation and bioavailability is complex [1,2] and still lacking under most conditions. For this reason, the majority of studies examining trace metal bioavailability have employed simplified models such as the free ion activity model (FIAM) or, more recently, the biotic ligand model (BLM) in an attempt to quantitatively relate chemical speciation to biological effects. Although the FIAM [3] and BLM [4] are based on the measurement of different fundamental parameters, that is, activity of the free-ion in solution (FIAM) or the metal adsorbed to sensitive sites at the biological surface (BLM), they both are steady-state models with similar assumptions and a similar conceptual framework (Fig. 1). Indeed, in any attempt to relate bulk solution measurements to bioavailability, it is necessary to take into account mass transport of the metal and metal complexes in the bulk solution; complexation and dissociation reactions in the immediate vicinity of the organism; and surface complexation to a cellular ligand (R_{cell}), which can either lead to the internalization of the metal or trigger a biological response.

In the FIAM and BLM, the entire steady-state process is simplified by coupling a rapid and reversible adsorption to membrane binding sites with an irreversible and rate-limiting internalization of the metal bound to the carrier (Eqn. 1) [3–5]

$$M^{Z+} + R_{cell} \xleftrightarrow{K_{M\text{-}R_{cell}}} M\text{-}R_{cell} \xrightarrow{k_{int}} \quad (1)$$

$$J_{int} = k_{int}\{M\text{-}R_{cell}\} \quad (2)$$

$$J_{int} = k_{int}K_{M\text{-}R_{cell}}\{R_{cell}\}[M^{Z+}] \quad (3)$$

where $K_{M\text{-}R_{cell}}$ is the conditional stability constant for the binding of the metal to sensitive sites at the cell surface (e.g., channels and carriers), k_{int} is the internalization rate constant, J_{int} is the metal internalization flux, $[M^{Z+}]$ is the free metal ion concentration in solution, and $\{M\text{-}R_{cell}\}$ is the metal bound to the sensitive sites. Equilibrium among the metal species in solution and those bound to the surface will be attained if transport across the biological membrane is rate-limiting [6,7]. In that case, for metal concentrations below saturation of the uptake sites, biological uptake fluxes will be directly proportional to any of the metal species in equilibrium (e.g., $\{M\text{-}R_{cell}\}$ in Eqn. 2 or $[M^{Z+}]$ in Eqn. 3). In the opposite case, for which biological internalization is rapid compared to either the physical transport or chemical reactivity of the metal [8,9], biological uptake fluxes will be better related to some other fraction of the metal species in solution (i.e., mobile or labile species) [1,8]. Although a biological transport limitation (assumption 1) is an extremely important requirement of the steady-state models [5,10], several other assumptions are required when using either the FIAM or the BLM: (2) the plasma membrane of the organism is the primary site of action of the trace metal; (3) no significant modification of the plasma membrane is assumed to occur (e.g., no degradation or synthesis of carriers); (4) no significant biological regulation is induced by binding to sensitive sites; (5) carrier ligands remain undersaturated; (6) internalization, if it occurs, is first order or pseudo first order; (7) the membrane surface is chemically

* To whom correspondence may be addressed (kevin.wilkinson@cabe.unige.ch).

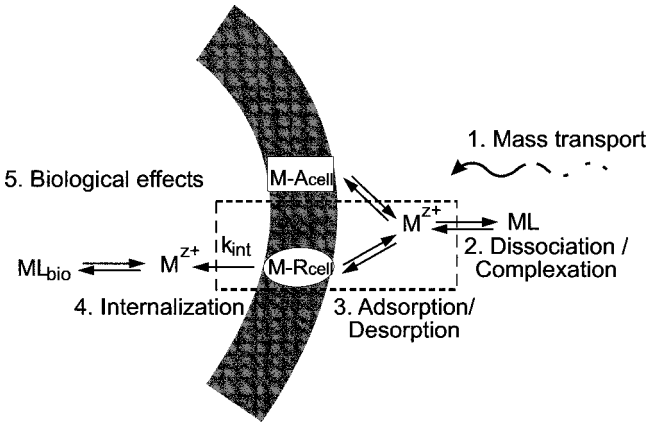

Fig. 1. Conceptual framework of the free ion activity model (FIAM) and biotic ligand model (BLM), including (1) mass transport of the free metal (M^{Z+}) and a hydrophilic complex (ML) in solution; (2) dissociation/complexation with a ligand in solution; (3) specific (M-R_{cell}) or nonspecific (M-A_{cell}) adsorption of the metal to the surface of the organism; (4) metal transport into the organism characterized by an internalization rate constant (k_{int}) and a subsequent reaction with an intracellular ligand (ML_{bio}); and (5) expression of the biological effect. The box identifies the reactions that are taken into account in the FIAM and BLM.

homogeneous (i.e., binding sites are independent of one another); and (8) the induced (acute) biological response is directly proportional to metal internalization fluxes (J_{int}) or to concentrations of the surface complex ({M-R_{cell}}).

The implications of these assumptions can be significant. Although carrier ligands are assumed to be involved in the internalization of many trace metals, they are not required; surface or channel mediated processes are generally sufficient for the models to hold (assumption 2). Researchers have tended to use short-term exposure experiments to increase the likelihood of assumptions 3 and 4 being applicable. Although first-order uptake kinetics (assumption 6) are predicted for undersaturated concentrations of the metal-carrier complex (assumption 5), especially in the case where conformational changes of the carrier are rate-limiting, they are not always observed, especially for essential metals such as Zn [9,11]. Assumption 7 is clearly an oversimplification because many different kinds of adsorptive sites have been identified on biological surfaces even for simple microorganisms [12,13]. In addition, several (not necessarily independent) transport routes have been found for metals such as Zn [9,14,15], Fe [16], and Ni [17]. Assumption 7 also implies that equilibrium constants will be valid (and constant) at variable metal:carrier ratios. Although assumption 8 is reasonable, very little research has been performed in that direction. Indeed, most current research on the biotic ligand model uses toxicity measurements to derive constants that are related, but not necessarily identical to the surface complexation constants [18–20].

Metal–metal interactions can be considered as antagonistic, with a potential reduction of bioavailability when both metals are present; synergistic, resulting in enhanced bioavailability of one metal due to the presence of another; or additive, where the observed effect is equivalent to the sum of the individual effects of the two metals [21]. When considering bioaccumulation (as opposed to toxicity) data, the steady-state models can only take into account antagonistic effects (i.e., reduction in biouptake or no effect [assumption 9]). In this case, competitor effects can be described in a similar manner for both internalization fluxes and the metal adsorbed to sensitive sites at the cell surface ({M-R_{cell}}) [22,23]

$$J_{int} = J_{max}\frac{K_{M\text{-}R_{cell}}[M^{Z+}]}{1 + K_{M\text{-}R_{cell}}[M^{Z+}] + K_{C\text{-}R_{cell}}[C]} \quad \text{and} \quad (4)$$

$$\{M\text{-}R_{cell}\} = \{R_{cell,tot}\}\frac{K_{M\text{-}R_{cell}}[M^{Z+}]}{1 + K_{M\text{-}R_{cell}}[M^{Z+}] + K_{C\text{-}R_{cell}}[C]} \quad (5)$$

where $K_{C\text{-}R_{cell}}$ is the stability constant for the adsorption of a competitor, C, to the same sensitive site as the metal; J_{max} is the maximum value of the metal internalization flux; and $\{R_{cell,tot}\}$ is the total concentration of sites. Equations 4 and 5 allow for a general prediction of the conditions in which the competitor will measurably decrease metal uptake. For low concentrations of trace metals, that is, $[M^{Z+}] < 1/K_{M\text{-}R_{cell}}$, which is generally the case in natural waters, J_{int} should be reduced by a factor $1/(1 + K_{C\text{-}R_{cell}}[C])$ in the presence of competitors.

The goal of this work is to examine the applicability of some of the key assumptions of the FIAM and the BLM on Pb and Zn bioaccumulation by the green alga *Chlorella kesslerii*. Lead and Zn were selected because of their variable toxicity and essentiality and because they are contrasting examples for which the steady-state models have been shown to succeed (Pb [24]) or fail (Zn [9]). In this study, metal uptake fluxes were related either to free-ion concentrations in solution ($[M^{Z+}]$, that is, basis of the FIAM, Eqn. 3) or to concentrations of the metal–transporter complex ({M-R_{cell}}, i.e., basis of the BLM, Eqn. 2). The roles of the competing ions (Ca, Cu, and Cd) and temperature were examined specifically in this respect. Results are discussed with respect to the potential applications of the models or their derivatives in complex environmental systems.

MATERIALS AND METHODS

Algal cultures

Chlorella kesslerii (University of Toronto Culture Collection, Toronto, ON, Canada, UTCC 266) was cultured in the Organization for Economic Cooperation and Development medium [25] in an incubation chamber at a constant temperature of 20°C, under a 12:12 h, light (50 μmol photon/m^2/s):dark regime and rotary shaking (100 rpm). Cells in their mid-exponential growth phase were harvested by gentle filtration (nitrocellulose, 3 μm), then washed and resuspended in an experimental medium containing 10^{-2} M *N*-[2-hydroxyethyl] piperazine-*N*′-[2-ethanesulfonic acid] (pH 7.0) for Zn or 10^{-2} M 2-[*N*-morpholino]ethanesulfonic acid (pH 6.0) for Pb bioaccumulation experiments, respectively.

Bioaccumulation experiments

Free metal concentrations were calculated by using MINEQL+ (Ver. 3.01a, Proctor & Gamble, Cincinnati, OH, USA) with updated stability constants (National Institute of Standards and Technology Critically Selected Stability Constants of Metal Complexes Database: Ver 5.0, Standard Reference Data Program, National Institute of Standards and Technology, Gaithersburg, MD, USA) and an ionic strength correction using the Davies equation. In a first set of experiments, free Zn was varied from 2×10^{-9} to 5×10^{-6} M in the absence ($[Zn^{2+}]$ ≈ 98% of total Zn) or presence of nitrilotriacetic acid. Nitrilotriacetic acid was added for $[Zn^{2+}] < 5 \times 10^{-7}$ M and a total [Zn] of 1 to 5×10^{-6} M. The [Pb] was varied from 5×10^{-9} to 5×10^{-6} M in the absence of added ligand. Under

Table 1. Summary of biotic ligand model (BLM) and free ion activity model (FIAM) parameters used to describe the trace metal uptake process

Abbreviation	Explanation	Experimental determination
J_{int}	Internalization flux, that is, equivalent to the metal uptake rate per unit surface area of the organism in contact with the bulk media [6,7]	Slope of the linear regression of the non-ethylenediaminetetraacetic acid (EDTA)–extractible metal content as a function of time (see Fig. 2) [24,26]
$\{M\text{-}R_{cell}\}$	Metal adsorbed to sites leading directly to uptake [6,26]. This metal-bound transporter may be considered as the biotic ligand. In reality, the biotic ligands also may include other intra- or extracellular sites [18,34]	*y*-intercept of the regression of non-EDTA–extractible metal content as a function of time (see Fig. 2) [9,24]
$\{M\text{-}A_{cell}\}$	Metal bound to adsorption sites on the cell wall and the membrane that do not lead to internalization [6]. Although often measured, these sites are not considered in the mathematical formulations of the FIAM and BLM (see Fig. 1)	EDTA–extractable metal content after a 1-min wash with 10^{-2} M EDTA [9,24,26]
$K_{M\text{-}R_{cell}}$	Equilibrium stability constant for the adsorption of metal to transport sites ($\{R_{cell}\}$; i.e., biotic ligand) [34]. This value assumes the formation of a 1 : 1 complex	Generally obtained from the reciprocal of the Michaelis–Menten constant (K_M) or from a Langmuir treatment of metal-bound transporter [7,24]
Permeability (P)	Internalization flux normalized by the concentration of free ion in the bulk solution	Ratio of J_{int} to $[M^{z+}]$; P should be constant for the FIAM to apply
k_{int}	Internalization rate constant relating J_{int} and $\{M\text{-}R_{cell}\}$ [5,7,8]. The k_{int} is assumed by the FIAM and BLM to be sufficiently small so as to limit uptake. The value of the constant depends on the type of transport pathway(s) involved (passive, active, and so on [6])	Ratio of J_{int} to $\{M\text{-}R_{cell}\}$ (see Eqn. 2); k_{int} should be constant for the BLM and FIAM to apply
Total adsorption	Total specific and nonspecific adsorption to the surface of an organ or organism [6,19]	$\{M\text{-}R_{cell}\} + \{M\text{-}A_{cell}\}$
Total body burden	Total metal concentration associated with an organism or an organ [19]	$\{M\text{-}R_{cell}\} + \{M\text{-}A_{cell}\} + \{M_{cell}\}$

these conditions (pH = 6.0 and ionic strength = 5 mM), 97% of the total Pb is present in the solution as the free lead ion, Pb^{2+}. In a second set of experiments, [Zn] and [Pb] were held constant at 10^{-6} M and competing ions (Ca, Cd, and Cu) were varied from 5×10^{-5} M to 10^{-3} M for Ca, from 5×10^{-6} M to 2×10^{-4} M for Cd, and from 10^{-8} M to 10^{-6} M for Cu. In a final set of experiments, the influence of temperature was examined by comparing bioaccumulation at 3 and 20°C.

In all cases, bioaccumulation was followed over short time periods (60 min for Pb and 25 min for Zn) to reduce variability due to biological regulation. Surface-bound (adsorbed) metal was distinguished from cellular metal by using a 1-min extraction with ethylenediaminetetraacetic acid (EDTA) [9,24,26]. The washing procedure was previously optimized for the nature of complexing ligands (nitrilotriacetic acid, *trans*-1,2-diaminocyclohexane-*N*,*N*,*N*′,*N*′-tetracetic acid, and EDTA) and the contact time of the ligand for Pb uptake by *C. kesslerii* [24]. The procedure was also verified for Zn. A 1-min wash was considered as optimal to minimize the significance of the Zn efflux [9] while maximizing Zn desorption. Cellular metal was determined after digestion of the filtered, EDTA-washed algae with concentrated ultrapure HNO_3. Adsorbed metal was quantified from the EDTA containing filtrate. Slopes from experimentally obtained temporal plots of the cellular metal concentrations (mol/cm^2) were employed to obtain metal uptake fluxes (mol/cm^2/s). The concentration of occupied metal transport sites was obtained from the *y*-intercepts of internalization curves after the EDTA extraction [24]. This relatively new technique has been shown to provide stability constants for the adsorption of metal to sensitive sites that are equivalent to those obtained from a Michaelis–Menten treatment of the uptake fluxes [24]. Furthermore, for identical conditions in the bulk medium but different concentrations of carrier ligands at the algal surface, this protocol has been shown to distinguish metal bound to transport sites from those involved in adsorption to sites that are not metabolically active [9]. Definitions of the important terms that are employed, including the methods used for their experimental determinations, are given in Table 1.

Cell densities, sizes, and surface areas were determined with a Coulter Multisizer II particle counter (Beckman Coulter, Nyon, Switzerland; 50 μm orifice). Experiments with Zn were performed with radiolabeled ^{65}Zn (Perkin-Elmer Life Science, Wellesley, MA, USA; specific activity of 185 GBq/g) representing <2% of the total Zn in the experimental media. The [^{65}Zn] was determined with a γ counter (Perkin-Elmer, Ueberlingen, Germany). The ratio of nonradiolabeled Zn: radiolabeled Zn was determined at the beginning of each experiment and used to transform the [^{65}Zn] into total dissolved [Zn]. Lead, Zn, and competing metals were quantified by using flame (Pye Unicam SP 9, Cambridge, UK) or electrothermal (Perkin-Elmer 4100) atomic absorption spectrometry or by inductively coupled plasma–mass spectrometry (Hewlett-Packard 4500, Palo Alto, CA, USA), depending on the concentration range.

Electrophoretic mobility determinations

To estimate modifications of the surface charge of *C. kesslerii* in the presence of Ca, electrophoretic mobilities (EPMs) were measured by laser Doppler velocimetry (Zetasizer 2000, Malvern Instruments, Worcertershire, UK). Electrophoretic mobilities were determined after a 35-min exposure of the algae to different concentrations of Ca. In these experiments, ionic strengths were kept constant (8×10^{-3} M) by addition of $NaNO_3$ to compensate for increasing $[Ca^{2+}]$ in solution. Zeta potential latex particle standards (Malvern) were used for calibration. The EPM data were treated by assuming that the algae behaved as rigid spheres with homogeneously distributed charges on the cell wall and a cellular diameter much larger

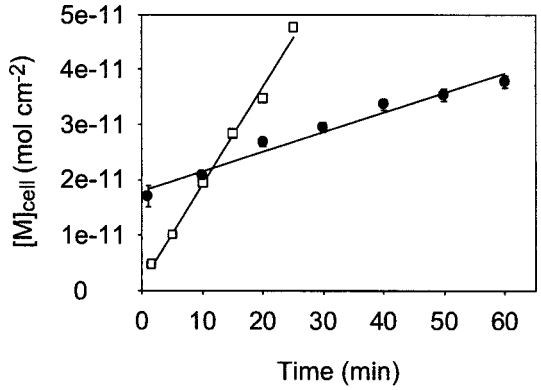

Fig. 2. Example of cellular metal concentrations as a function of the accumulation time for 10^{-6} M of Pb (●) and Zn (□). The slope is used to calculate the internalization uptake flux (J_{int}), whereas the intercept is employed to determine the concentration of transporter-bound metal ({M-R_{cell}}). In this case, $J_{int} = 1.8 \times 10^{-12}$ and 3.6×10^{-13} mol/cm²/min and {M-R_{cell}} = 1.6×10^{-12} and 1.8×10^{-11} mol/cm² for Zn and Pb, respectively.

than the Debye length [27]. In this manner, it was possible to estimate the cell zeta potential by using Smoluchowski's equation [28]. Furthermore, by estimating that the shear plane was a few water layers from the cell surface, a first approximation of the algal surface potential (ψ_0) could be obtained as a function of [Ca^{2+}]. The ratio between the metal immediately adjacent to the charged algal surface and that in the bulk solution was then estimated by using Boltzmann's law [27]

$$\frac{\{\text{M-R}_{\text{cell}}\}}{[\text{M}]} = \exp\left(\frac{zF\psi_0}{RT}\right) \quad (6)$$

where z is the algebraic charge number of M, T is the absolute temperature, F is the Faraday constant, and R is the gas constant.

General data treatment

At each time point, a mass balance was performed by taking into account dissolved, adsorbed, and cellular concentrations of the metal. Data were rejected if the mass balance exceeded a 10% variation from the initial dissolved concentration. Each experiment was repeated a minimum of two times. For bioaccumulation experiments performed in the presence of competitors, control experiments with Zn or Pb in the absence of competing ions were performed in parallel. Data were normalized with respect to the measured dissolved bulk metal concentrations rather than nominal metal concentrations.

RESULTS AND DISCUSSION

Verification of the steady-state assumption for Pb and Zn uptake

Figure 2 gives a typical example of the bioaccumulation results for 10^{-6} M metal at a relatively high cellular density of 1.5×10^6 cells/ml. For both metals, the surface normalized concentration inside the cell increased linearly with time, implying that internalization fluxes and the concentration of metal bound to the transport sites were constant (see Eqn. 2). For 10^{-6} M free metal in the bulk solution, adsorbed Pb (1.2×10^{-10} mol/cm²) was twice that of adsorbed Zn (6.0×10^{-11} mol/cm²), whereas internalization fluxes (i.e., slopes in Fig. 2) were approximately fivefold smaller for Pb as compared to Zn. Maximal Pb adsorption obtained from a Langmuir isotherm was 6.6×10^{-10} mol/cm² for bulk [Pb^{2+}] > 2×10^{-5} M [26]. On the other hand, saturation of Zn adsorption did not occur below 10^{-3} M Zn^{2+} [10]. For both metals, when algae were added to the experimental solutions, a rapid initial decrease in the metal concentration in the bulk medium was observed, followed by a stable dissolved concentration. Mass balance calculations revealed that the decrease was due to the initial nonspecific adsorption of metal to the biological surface, whereas the plateau value was due to a pseudoequilibrium between the bulk solution and the algal surface [6,7,9,24]. After the initial decrease of metal, biouptake observations are therefore in qualitative agreement with either of the steady-state models (FIAM or BLM).

Nonetheless, the steady-state models are only applicable if biological transport limits the cellular metal uptake flux. In the case where mass transport of the metal in solution is limiting, the maximum diffusive flux due to radial diffusion (J_{diff}^{max}) can also give a similar dependence on the free ion

$$J_{\text{diff}}^{\max} = \frac{\overline{D} \cdot C_{\text{bulk}}}{R} \quad (7)$$

where $\overline{D}$ is the weighted mean diffusion coefficient for the metal [29], C_{bulk} is the concentration of metal in the bulk solution, and R corresponds to the radius of the organism (~ 2.0 μm for *C. kesslerii*). Under the conditions examined here, the maximal diffusive supply of free ions to algal surface (5.3×10^{-11} and 4.0×10^{-11} mol/cm²/s for Pb and Zn, respectively) was higher by several orders of magnitude than the observed uptake fluxes at 10^{-6} M [M^{z+}] (5.9×10^{-15} and 3.0×10^{-14} mol/cm²/s for Pb and Zn, respectively). Although no precise data are available for the rates of Zn and Pb adsorption by the specific sites of the membrane surface, calculations based on the Eigen mechanism [30] (rate-limiting loss of water from the hydration sphere of the cation) suggest that reaction kinetics at the membrane surface are also many orders of magnitude faster that the observed internalization fluxes. Each of the previous considerations supports the use of the steady-state models to predict Zn or Pb uptake.

Applicability of the BLM and FIAM in absence of competitors

As mentioned above, an underlying assumption of both the FIAM and BLM is that internalization fluxes (Eqns. 2 and 3) should be directly proportional to either [M^{z+}] or {M-R_{cell}}. In other words, membrane permeability ($P = J_{int}/[M^{z+}] = k_{int} \cdot K_{M\text{-}R_{cell}} \cdot \{R_{cell}\}$) or the internalization rate constant ($k_{int} = J_{int}/\{\text{M-R}_{\text{cell}}\}$) should be constants. Bioaccumulation experiments were performed at constant pH and ionic strength by varying the concentration of free metal in the bulk solution. When [Pb^{2+}] increased from 5×10^{-9} to 5×10^{-6} M, uptake fluxes also increased by three orders of magnitude, confirming the first-order relationship between the free ion concentration and the internalization flux J_{int}, as predicted by the FIAM (slope of 1 in Fig. 3a; see Eqn. 3). In other words, for Pb, membrane permeability ($J_{int}/[Pb^{2+}]$) was constant and equal to $(3.3 \pm 0.5) \times 10^{-6}$ cm/s. The BLM was verified by determining whether k_{int} was constant as a function of the free ion concentration (Fig. 3b). For Pb, k_{int} ($J_{int}/\{\text{Pb-R}_{\text{cell}}\}$) was indeed constant, equal to $(4.9 \pm 1.8) \times 10^{-4}$/s for [$Pb^{2+}$] from 5×10^{-9} to 5×10^{-6} M.

In contrast, for Zn, neither the FIAM nor the BLM were able to predict metal internalization fluxes. The J_{int} increased by approximately two orders of magnitude for a four order of magnitude increase of [Zn^{2+}] (slope of 0.7 in Fig. 3a). Furthermore, k_{int} ($J_{int}/\{\text{Zn-R}_{\text{cell}}\}$) was variable for different con-

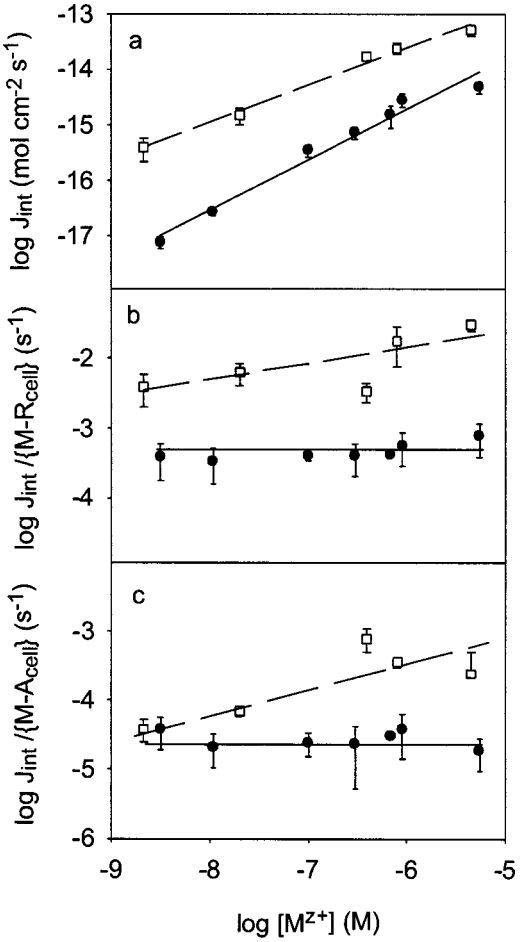

Fig. 3. Lead (●) and Zn (□) bioaccumulation data in the absence of competitors. (**a**) Internalization fluxes (J_{int}) and the linear regressions (solid line for Pb with a slope of 1.0 and $r^2 = 0.99$; dashed line for Zn with a slope of 0.7 and $r^2 = 0.99$); (**b**) values of the internalization rate constant obtained by dividing the internalization flux by the transporter bound metal ({M-R_{cell}}); and (**c**) internalization fluxes divided by adsorbed metal ({M-A_{cell}}). Error bars represent the standard deviations from two to four experiments.

centrations of [Zn^{2+}] in the bulk solution (Fig. 3b), increasing fivefold for [Zn^{2+}] ranging from 2×10^{-9} to 5×10^{-6} M. A slope of 1 in Figure 3a would have supported the assumption that the interaction of Zn occurred via a single homogeneous site. A reasonable interpretation of the lower slope could be due to the chemical heterogeneity of binding sites, similar to results commonly obtained for natural organic matter [31]. Because Zn bioaccumulation is mediated by several possible uptake pathways with different affinities involving both active and passive transport [9,14,15] neither the first-order uptake kinetics (assumption 6) nor the single site approach (e.g., Langmuir, assumption 7) are appropriate in this case. Indeed, for Zn, values of k_{int} and $K_{Zn\text{-}R_{cell}}$ are dependent upon the surface coverage and the [Zn^{2+}] in the bulk solution. For example, for 10^{-6} M Zn^{2+}, k_{int} was $(1.8 \pm 0.8) \times 10^{-2}$/s and $K_{Zn\text{-}R_{cell}} = 10^{4.3}$ M^{-1}, whereas at 10^{-9} M Zn^{2+}, k_{int} was substantially lower $(3.9 \pm 3.2) \times 10^{-3}$/s and $K_{Zn\text{-}R_{cell}}$ was substantially larger ($10^{5.7}$ M^{-1}). Values of $K_{Zn\text{-}R_{cell}}$ determined in this manner were nonetheless of the same order of magnitude as values observed for *Daphnia magna* ($10^{5.3}$ to $10^{5.4}$ M^{-1} at pH 6.8 [32]) and for *C. kesslerii* at pH 6.8 ($10^{4.1}$ M^{-1}) [33]. Indeed, the occurrence of specialized and multiple transport routes in concert with a well-developed Zn regulatory system are likely the main reasons for the failure of the BLM and FIAM to predict Zn uptake fluxes even under these simple, well-controlled conditions. Such a situation would be more likely for the essential metals, including Zn, than for purely toxic metals (e.g., Pb) because of the capacity of the organism to regulate cellular concentrations [6,7]. Although more complex adsorption models are available to account for surface heterogeneity, polyelectrolytic effects, and multiple sites, none of these purely mathematical treatments can easily account for an internal Zn homeostasis [7,14].

Although the concentrations of M-R_{cell} (Fig. 3b) more closely resemble the biotic ligand of the BLM, a much more involved procedure is required for their determination [26] as compared to total adsorbed [19,34] or total cellular metal concentrations. Indeed, in many studies that apply the BLM, the biotic ligand concentration is estimated from the sum of the extracellular and intracellular binding sites [24] or by considering an entire organ such as the fish gill (i.e., total body burden or total adsorption). Concentrations of metal adsorbed to the sensitive sites on the organism are necessarily smaller than total adsorbed concentrations ({M-A_{cell}}). Nonetheless, because of the frequency and facility of the determination of {M-A_{cell}}, the relationship between J_{int} and total adsorbed metal also was verified here. As seen for previous parameters (Fig. 3a and b), the ratio J_{int}/{Pb-A_{cell}} was constant across the Pb concentrations in the bulk solution (Fig. 3c), with a proportionality constant that was significantly smaller than k_{int}, that is, $(2.9 \pm 1.1) \times 10^{-5}$/s and without any real physical meaning. In addition, for both Pb and Zn, the values of the conditional stability constants for the nonspecific adsorption ($K_{M\text{-}A_{cell}}$) were significantly smaller (~50×) than the values obtained for adsorption to metal transporters. These observations are not surprising given the much larger number of weakly adsorbing sites (cell wall components, membrane phospholipids, and others) as compared to transport sites. As above, for Zn, the ratio J_{int}/{Zn-A_{cell}} was variable, increasing 20-fold for [Zn^{2+}] ranging from 2×10^{-9} to 5×10^{-6} M.

Applicability of the BLM and FIAM in the presence of competitors

The BLM offers the practical possibility of taking directly into account the antagonistic competition of chemicals (e.g., H^+ and other cations) with the biotic ligand. Both the FIAM and the BLM predict that the competitor will either decrease or have no effect on cellular metal concentrations. For 10^{-6} M metal in the bulk solution and a value of $K_{Ca\text{-}R_{cell}} = 10^{4.2}$ M^{-1}, Pb uptake fluxes would be predicted to decrease for [Ca^{2+}] $> 5 \times 10^{-5}$ M (Eqn. 4), whereas no measurable effect on the maximum uptake flux would be expected. In a similar manner for 10^{-6} M Zn^{2+}, significant decreases in the Zn uptake fluxes are predicted for [Ca^{2+}] $> 2.5 \times 10^{-6}$ M.

Experimental results revealed that when [Ca^{2+}] exceeded that employed in the initial growth medium, that is, 10^{-4} M, a quantitative decrease in the Pb internalization fluxes was observed in accordance with the theoretical predictions. For 10^{-6} M [Pb^{2+}], internalization fluxes decreased about 20-fold and {Pb-R_{cell}} decreased about twofold for an increase of [Ca^{2+}] from 5×10^{-5} to 10^{-3} M (Fig. 4a, circles). Moreover, for a systematic variation of [Pb^{2+}] in the presence of 5×10^{-4} M Ca^{2+}, Ca^{2+} behaved as a competitive inhibitor with a conditional binding constant of $K'_{Ca\text{-}R_{cell}}$ of $10^{4.6}$ M^{-1} (pH 6.0), about 10 times lower than the stability constant for the binding of Pb to transport sites ($K'_{Pb\text{-}R_{cell}} = 10^{5.5}$ M^{-1}) [26]. On the other hand, Zn-normalized internalization fluxes decreased only

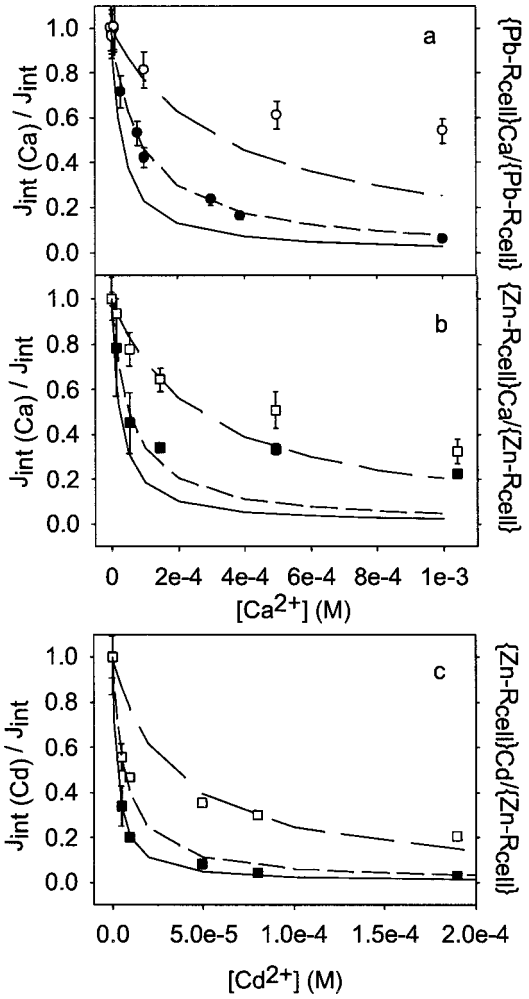

Fig. 4. Fits of experimentally determined, normalized transporter bound metal ({M-R_{cell}}; open symbols) and internalization fluxes (J_{int}; solid symbols) in the presence of the competitors, calculated by using Equations 4 and 5. (**a**) Pb–Ca interaction (circles): 10^{-6} M Pb, log $K_{Pb\text{-}R_{cell}}$ = 5.4 and (**b**) Zn–Ca interaction (squares): 10^{-6} M Zn, log $K_{Zn\text{-}R_{cell}}$ = 4.3. In both cases, log $K_{Ca\text{-}R_{cell}}$ was 4.6 (long dashed lines), 4.2 (short dashed lines), and 3.6 (solid lines); (**c**) Zn–Cd interaction: 10^{-6} M Zn, log $K_{Zn\text{-}R_{cell}}$ = 4.3 with a log $K_{Cd\text{-}R_{cell}}$ of 5.6 (long dashed lines), 5.2 (short dashed lines), and 4.5 (solid lines). Both J_{int} and {M-R_{cell}} in the presence of competitor are normalized to the values in the absence of competitor. Error bars represent standard deviations (n = 3).

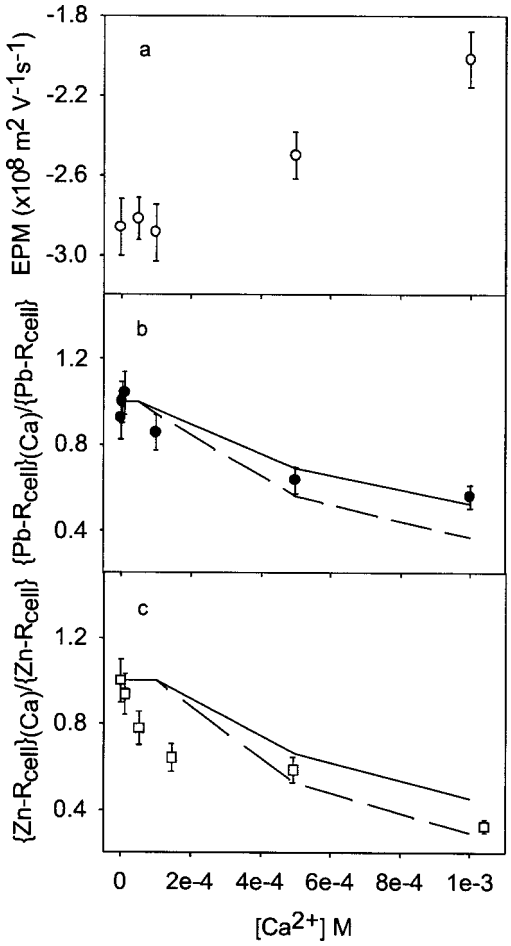

Fig. 5. (**a**) Variation of the electrophoretic mobility (EPM) ± standard deviation for *Chlorella kesslerii* as a function of [Ca^{2+}] (pH 6.0, contact time 35 min). Calculated surface concentrations ({M-R_{cell}}$_{Ca}$) in the presence of Ca normalized to those in its absence ({M-R_{cell}}), for (**b**) Pb (●) and (**c**) Zn (□). Theoretical predictions are based upon the Boltzmann equation (Eqn. 6 [27]) for a potential value calculated at 0.5 nm (solid line) and 2.0 nm (dashed line) from the algal surface. Experimentally determined values are given by open circles.

fourfold in the presence of a 1,000-fold excess of Ca (Fig. 4b, solid symbols), showing a weaker competitive effect of Ca on Zn, as compared to Pb biouptake. Similarly, a very small decrease in normalized {Zn-R_{cell}}, from 1.0 to 0.3 × 10^{-3} cm (Fig. 4b, open symbols), was observed in the presence of 10^{-3} M Ca.

Theoretical predictions and experimentally determined values of J_{int} and {M-R_{cell}} in the presence of competitors were normalized to data in their absence. Figure 4 provides three fits of the competition Equations 4 and 5 with experimental data obtained for the internalization fluxes and metal-bound carrier concentrations in presence of Ca (Pb and Zn) and Cd (Zn). For a given stability constant, theoretical curves for the normalized flux and carrier-bound metal should be superimposed. A reasonably quantitative prediction of the magnitude of the Ca effect on the experimentally determined Pb uptake fluxes (Fig. 4a, short dashed line) was obtained for $K_{Ca\text{-}R_{cell}}$ = $10^{4.2}$ M^{-1}), a value similar to that reported by Slaveykova and Wilkinson [24]. In contrast for Zn, J_{int} was successfully modeled only for [Ca] < 10^{-4} M (Fig. 4b, short dashed lines). A reasonable fit of modeled and experimental data for the carrier-bound Pb and Zn (Eqn. 5, $K_{Pb\text{-}R_{cell}}$ = $10^{5.5}$ M^{-1} and $K_{Zn\text{-}R_{cell}}$ = $10^{4.3}$ M^{-1}) was only possible at low [Ca^{2+}] (< 10^{-4} M) when using $K_{Ca\text{-}R_{cell}}$ = $10^{3.6}$ M^{-1} (Fig. 4a and b, long dashed lines).

The more pronounced difference between the experimentally determined and calculated values of {M-R_{cell}} at higher [Ca^{2+}] was postulated to be due to changes in the membrane surface charge in the presence of the higher concentrations of Ca. Indeed, EPM measurements confirmed that an increase in [Ca^{2+}] from 10^{-5} M to 10^{-3} M resulted in lower values of negative EPM (Fig. 5a) at both pH 6.0 and 7.0. Given that the experiments were performed at constant ionic strength and pH, it can be assumed that the EPM was directly related to the cell surface potential and thus the surface charge. For example, at pH = 6.0, it is possible to estimate an algal surface potential of −41.5 mV in the absence of Ca and −33.3 mV in the presence of 10^{-3} M Ca (Eqn. 6). In the presence of a constant concentration of metal in the bulk solution, a smaller surface potential would result in a decreased concentration of Pb and

Zn at the cell surface. In this manner, the ratio between surface and bulk Pb can be shown to decrease by a factor of approximately two in the presence of 10^{-3} M Ca. When surface potentials were used to correct for Ca effects by using the Boltzmann equation (Eqn. 6), relatively good agreement between experimentally measured and theoretically predicted {Pb-R_{cell}} was obtained at high [Ca^{2+}] (Fig. 5b). On the other hand, prediction of the role of Ca on {Zn-R_{cell}} was only successful when [Ca^{2+}] was higher than 5×10^{-4} M (Fig. 5c). These results suggested that Ca was not only directly reducing binding through competition for the sensitive sites but also might have had an indirect effect on ion transport.

Indeed, in the absence of Ca in the experimental solutions, cells that were preincubated in a growth medium containing 1×10^{-4} M Ca^{2+} had a higher permeability to Pb (3.3×10^{-6} cm/s) than cells cultivated in 8×10^{-4} M Ca^{2+} (1.7×10^{-6} cm/s). The observed difference in permeability suggested that either Ca dissociation kinetics were extremely slow or that Ca^{2+} modified the membrane surface through a possible modulated expression of the common transport pathway for Pb and Ca [24].

Unlike Ca, Cd had no observable competitive effect on Pb internalization fluxes for a 10-fold excess of competitor. On the other hand, for a relatively small 10-fold excess in [Cd], Zn uptake fluxes decreased by a factor four, whereas carrier-bound and total adsorbed Zn decreased by factors of two and three, respectively. For a 200-fold excess of Cd, the normalized uptake fluxes decreased by 320-fold, whereas the normalized {Zn-R_{cell}} only decreased by a factor of five (Fig. 4c). Cadmium is known to be a competitor for both Zn uptake and enzymatic site binding [35–37] because of its similar charge, coordination, and ligand preferences. Therefore, Cd has a stronger competitive effect for Zn than does Ca, with a resulting higher value of $K_{Cd\text{-}R_{cell}} = 10^{5.6}$ M^{-1} required to predict the measured uptake fluxes (Fig. 5c, solid points and solid line). Nonetheless, as observed for the competitive effect of Ca above, {Zn-R_{cell}} could not be modeled at high [Cd^{2+}]. Below 10^{-5} M Cd^{2+}, a value of $K_{Cd\text{-}R_{cell}} = 10^{5.2}$ M^{-1} was required to quantitatively predict {Zn-R_{cell}} (Fig. 4c, short and long dashed lines).

In large part, the inability to model Zn competition by Cd and Ca can be explained by the active nature of Zn uptake (as opposed to the purely passive nature of Zn adsorption to the carriers). In this case, values of k_{int} were not constant in the range of concentrations of the competitors that were studied. As discussed previously, Zn homeostasis is important in that the organism can rapidly modify its uptake fluxes in response to the external environment [9]. Furthermore, Cd is known to bind to specific enzymatic sites meant for Zn [36], partially altering their biochemical activity leading to a partial inhibition of specific Zn transporters and an important reduction of Zn internalization fluxes.

As mentioned above, a key assumption of the BLM is that the metal bound to a sensitive site, in this case {Zn-R_{cell}}, is directly related to the observed biological effect, that is estimated here by the value of J_{int} (Eqn. 2). In the presence of competitor, the direct first-order relationship between J_{int} and {M-R_{cell}} was not observed. Furthermore, it was not possible to fit measured values of {M-R_{cell}} and J_{int} by using the same set of stability constants. Although the observed differences might be partially due to discrepancies in the analytical determination of {M-R_{cell}}, the lack of model agreement, even when employing precise values of J_{int}, strongly suggested a fundamental flaw with one or more of the model assumptions.

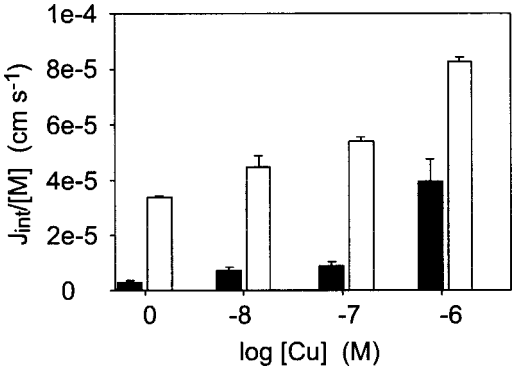

Fig. 6. Competitive effect of Cu on Pb (■) and Zn (□) internalization fluxes after normalization by Pb and Zn concentrations in the bulk medium. [Pb^{2+}] and [Zn^{2+}] were nominally 10^{-6} M. Error bars represent standard deviations from two or three experiments.

Neither steady-state model could predict the effect of Cu on the uptake process. Contrary, to model expectations, Pb and Zn internalization fluxes were strongly increased by the presence of Cu (Fig. 6). In fact, the addition of Cu to the experimental medium increased metal uptake fluxes even when present at concentrations that were 100 times lower than the studied metal (Pb or Zn). In this case, Cu additions did not significantly affect {M-R_{cell}} (variations <20%). A similar synergistic role of Cu has been observed for the bioaccumulation of Zn, Pb, and other metals for several different aquatic organisms [24,38]. It is possible to speculate that the Cu affected the physiology of the organism, although no metabolic influence of Cu, evaluated by a 10-min incubation with $NaH^{14}CO_3$, was seen here (data not shown). On the other hand, a twofold decrease in ^{14}C D-sorbitol accumulation (10-min contact time), indicative of a decrease in overall (lipidic) membrane permeability, was observed after exposure to 10^{-6} M Cu^{2+}. The major toxicological effects of Cu are known to include a disruption of membrane integrity that is associated with an increased cation membrane permeability and H^+-adenosine triphosphatase activity [39,40].

Temperature effects on Pb and Zn bioaccumulation

Although both the entropy and enthalpy of reaction may vary with temperature for metal–protein interactions [41], binding to membrane receptors is generally considered an exothermic process that is driven primarily by positive entropy changes [42]. In such a case, for a decrease in temperature, small changes would be expected for equilibrium binding data whereas large reductions of the internalization fluxes might occur. The validity of the steady-state approaches was therefore tested by verifying if membrane permeability ($J_{int}/[M^{Z+}]$; FIAM), and the internalization rate constant ($J_{int}/\{M\text{-}R_{cell}\}$; BLM), remained constant across an environmentally relevant temperature range. For both Zn and Pb, internalization fluxes increased significantly for a temperature increase from 3 to 20°C (Table 2). Temperature effects were more important for Pb (fivefold increase in J_{int}) than for Zn (twofold increase), probably reflecting that metabolic activity was less implicated in Pb transport than for the strongly regulated Zn transport. A decrease in temperature also decreased the concentration of carrier-bound metal ({M-R_{cell}}). For Pb, the decrease in J_{int} greatly outweighed the decrease in {Pb-R_{cell}}, resulting in an

Table 2. Effect of the temperature on the biouptake of 10^{-6} M [Pb^{2+}] and [Zn^{2+}]. Data are given as internalization fluxes over free metal concentrations in the bulk solution (i.e., membrane permeability) or metal bound to transporters (i.e., internalization rate constant). Data are mean values ± standard deviation (SD); $n = 3$

Metal	T (°C)	Membrane permeability ($J_{int}/[M^{z+}]$) ± SD (cm/s)	Internalization rate constant ($J_{int}/\{M\text{-}R_{cell}\}$) ± SD ($s^{-1}$)
Zn	3	$(3.2 \pm 0.3) \times 10^{-4}$	$(9.8 \pm 0.6) \times 10^{-2}$
	20	$(7.1 \pm 0.4) \times 10^{-4}$	$(9.7 \pm 0.9) \times 10^{-2}$
Pb	3	$(4.3 \pm 0.9) \times 10^{-7}$	$(3.6 \pm 0.9) \times 10^{-4}$
	20	$(3.4 \pm 0.5) \times 10^{-6}$	$(7.0 \pm 1.6) \times 10^{-4}$

overall decrease in k_{int} from 7.0×10^{-4} to 3.6×10^{-4}/s. For Zn, both J_{int} and $\{Zn\text{-}R_{cell}\}$ decreased in parallel in a manner to maintain k_{int} constant at $(1.7 \pm 0.3) \times 10^{-3}$/s. In that case, BLM predictions with $\{Zn\text{-}R_{cell}\}$ would be more reflective of metal internalization fluxes than those made on the basis of [Zn^{2+}] (FIAM).

Other effects

In the preceding discussion, we have examined the role of competing ions and temperature on Zn and Pb internalization fluxes. Neither effect could be predicted quantitatively on the basis of either the FIAM or the BLM. Other exceptions to the FIAM and BLM have been thoroughly discussed by Campbell [5] and Campbell et al. [10], and others [23,24]. These include the role of small metabolizable, anionic ligands on the uptake process [43], the uptake of lipophilic complexes [44], the presence of multiple uptake routes [7,9,14,16], the influence of humic substances [45,46], and the role of the hydrodynamic regime [47]. Despite the numerous exceptions, it is not the goal of this paper to suggest that the BLM or the FIAM are not useful constructs that can enable a better understanding of the trace metal uptake process and lead to better, more quantitative predictions in the field. Nonetheless, the above considerations and data suggest that the BLM and FIAM may be most useful for predicting the uptake of nonessential metals under reasonably controlled conditions only. The inability of these models to explain the variation of Pb and Zn uptake with temperature or the competition with Cu are serious drawbacks that are sure to limit their application to field conditions. Indeed, the ubiquitous nature of Cu and natural organic matter and the lack of a controlled temperature in the field implies that trace metal uptake fluxes will be highly variable in natural waters and most often independent of [M^{z+}]. In any case, further research will be required to fully incorporate these effects into these the FIAM, BLM, or other similar models before any quantitative regulatory monitoring of trace metal speciation should be seriously considered.

CONCLUSION

To verify the applicability of the FIAM and BLM, experimentally determined uptake fluxes were related to free metal ion concentrations and metals bound to transport sites. It was shown that, in the absence of competitors, both the FIAM and the BLM can be applied to describe Pb biouptake by *C. kesslerii*, whereas the models failed to explain the experimental data obtained for Zn. Although Zn internalization fluxes could not be predicted in the presence of Ca, Pb internalization fluxes were reasonably well modeled in the presence of Ca and Zn in the presence of Cd. On the other hand, to model the metal bound to the sensitive sites ($\{M\text{-}R_{cell}\}$) in the presence of high concentrations of divalent cations, it was necessary to take into account modifications in the algal surface charge, membrane permeability, the nature of transport system, and physiological effects, parameters generally not taken into account in the simplified models. Neither the FIAM nor BLM were able to describe the observed synergistic effects of Cu on Zn and Pb uptake fluxes. Finally, temperature was demonstrated to reduce Pb uptake fluxes to a greater extent than it reduced binding to transport sites.

Acknowledgement—This work was supported, in part, by the European Union 5th framework Biospec project (EVK1-CT-2001-00086). We are grateful to Michel Martin and Marco Tuveri for technical assistance. Helpful critical comments on earlier drafts of the manuscript were provided by Heliana Kola, Isabelle Worms, and two anonymous reviewers.

REFERENCES

1. Van Leeuwen HP. 1999. Metal speciation dynamics and bioavailability: Inert and labile complexes. *Environ Sci Technol* 33:3743–3748.
2. Pinheiro J-P, van Leeuwen HP. 2001. Metal speciation dynamics and bioavailability. 2. Radial diffusion effects in the microorganism range. *Environ Sci Technol* 35:890–900.
3. Morel FMM. 1983. *Principles of Aquatic Chemistry*. Wiley-Interscience, New York, NY, USA.
4. Pagenkopf G. 1983. Gill surface interaction model for trace-metal toxicity to fishes: Role of complexation, pH, and water hardness. *Environ Sci Technol* 17:342–347.
5. Campbell PGC. 1995. Interactions between trace metals and aquatic organisms: A critique of the free ion activity model. In Tessier A, Turner DR, eds, *Metal Speciation and Bioavailability in Aquatic Systems*, Vol 3. IUPAC Series on Analytical and Physical Chemistry of Environmental Systems. John Wiley, New York, NY, USA, pp 45–102.
6. Hudson RJM. 1998. Which aqueous species control the rates of trace metal uptake by aquatic biota? Observations and predictions of nonequilibrium effects. *Sci Total Environ* 219:95–115.
7. Sunda WG, Huntsman SA. 1998. Processes regulating cellular metal accumulation and physiological effects: Phytoplankton as model systems. *Sci Total Environ* 219:165–181.
8. Hudson RJM, Morel FMM. 1993. Trace metal transport by marine microorganisms: Implications of metal coordination kinetics. *Deep-Sea Res Part I Oceanogr Res Pap* 40:129–150.
9. Hassler CS, Wilkinson KJ. 2003. Failure of the biotic ligand and free-ion activity models to explain zinc bioaccumulation by *Chlorella kesslerii*. *Environ Toxicol Chem* 22:620–626.
10. Campbell PGC, Errecalde O, Fortin C, Hiriart-Baer VP, Vigneault B. 2002. Metal bioavailability to phytoplankton—Applicability of the biotic ligand model. *Comp Biochem Physiol Toxicol Pharmacol* 133:185–202.
11. Mirimanoff N, Wilkinson KJ. 2000. Regulation of Zn accumulation by a freshwater gram-positive bacterium (*Rhodococcus opacus*). *Environ Sci Technol* 34:616–622.
12. Crist RH, Oberholser K, Shank N, Nguyen M. 1981. Nature of binding between metallic ions and algal cell walls. *Environ Sci Technol* 15:1212–1217.
13. Xue H-B, Stumm W, Sigg L. 1988. The binding of heavy metals to algal surfaces. *Water Res* 22:917–926.

14. Van Ho A, Mc Vey Ward D, Kaplan J. 2002. Transition metal transport in yeast. *Annu Rev Microbiol* 56:237–261.
15. Sunda WG, Huntsman SA. 1992. Feedback interactions between zinc and phytoplankton in seawater. *Limnol Oceanogr* 37:25–40.
16. Koester W. 2004. Transport of solutes across biological membranes: prokaryotes. In van Leeuwen HP, Koester W, eds, *Physicochemical Kinetics and Transport at Biointerfaces*. John Wiley, New York, NY, USA, pp 271–336.
17. Eitinger T, Mandrand-Berthelot M-A. 2000. Nickel transport systems in microorganisms. *Arch Microbiol* 173:1–9.
18. Heijerick DG, De Schamphelaere KAC, Janssen CR. 2002. Biotic ligand model development predicting Zn toxicity to the alga *Pseudokirchneriella subcapitata* possibilities and limitations. *Comp Biochem Physiol Toxicol Pharmacol C* 133:243–258.
19. Santore RC, Di Toro DM, Paquin PR, Allen HE, Meyer JS. 2001. Biotic ligand model of the acute toxicity of metals. 2. Application to acute copper toxicity in freshwater fish and *Daphnia*. *Environ Toxicol Chem* 20:2397–2402.
20. Brown PL, Markich SJ. 2000. Evaluation of the free ion activity model of metal- organism interaction: Extension of the conceptual model. *Aquat Toxicol* 51:177–194.
21. Babich H, Stotzky G. 1983. Influence of chemical speciation on the toxicity of heavy metals to the microbiota. *Adv Environ Sci Technol* 13:1–46.
22. Galceran J, van Leeuwen HP. 2004. Dynamic of biouptake processes. The role of transport, adsorption and internalization. In van Leeuwen HP, Koester W, eds, *Physicochemical Kinetics and Transport at Biointerfaces*. John Wiley, New York, NY, USA, pp 147–204.
23. Wilkinson KJ, Buffle J. 2004. Critical evaluation of physicochemical parameters and processes for modeling the biological uptake of trace elements in environmental (aquatic) systems. In van Leeuwen HP, Koester W, eds, *Physicochemical Kinetics and Transport at Biointerfaces*. John Wiley, New York, NY, USA, pp 445–533.
24. Slaveykova VI, Wilkinson KJ. 2002. Physico-chemical aspects of lead bioaccumulation by *Chlorella vulgaris*. *Environ Sci Technol* 36:969–975.
25. Organization for Economic Cooperation and Development. 1984. Algal growth inhibition test. Guideline 201. Paris, France.
26. Bates SS, Tessier A, Campbell PGC, Buffle J. 1982. Zinc adsorption and transport by *Chlamydomonas variabilis* and *Scenedesmus subspicatus* (Chlorophyceae) grown in semicontinuous culture. *J Phycol* 18:521–529.
27. Kleijn JM, van Leeuwen HP. 2000. Electrostatic and electrodynamic properties of biological interphases. In Baszkin A, Norde W, eds, *Physical Chemistry of Biological Interfaces*. Marcel Dekker, New York, NY, USA, pp 49–84.
28. Ohshima H. 1998. Electrical double layer. In Ohshima H, Furusawa K, eds, *Electrical Phenomena at Interfaces—Fundamentals, Measurements and Applications*. Marcel Dekker, New York, NY, USA, pp 1–55.
29. Kariuki S, Dewald HD. 1996. Evaluation of diffusion coefficients of metallic ions in aqueous solutions. *Electroanalysis* 8:307–312.
30. Morel FMM, Hering JG. 1995. *Principles and Applications of Aquatic Chemistry*. John Wiley, New York, NY, USA.
31. Buffle J. 1988. *Complexation Reactions in Aquatic Systems. An Analytical Approach*. Ellis, Horwood, Chichester, UK.
32. Heijerick DG, De Schamphelaere KAC, Janssen CR. 2002. Predicting acute zinc toxicity for *Daphnia magna* as a function of key water chemistry characteristics: Development and validation of a biotic ligand model. *Environ Toxicol Chem* 21:1309–1315.
33. Ting YP, Lawson F, Prince IG. 1989. Uptake of cadmium and zinc by the alga *Chlorella vulgaris*: Part I. Individual ion species. *Biotechnol Bioeng* 34:990–999.
34. Di Toro DM, Allen HE, Bergman HL, Meyer JS, Paquin PR, Santore RC. 2001. Biotic ligand model of the acute toxicity of metals. 1. Technical basis. *Environ Toxicol Chem* 10:2383–2396.
35. Price NM, Morel FMM. 1990. Cadmium and cobalt substitution for zinc in a marine diatom. *Nature (Lond)* 344:658–660.
36. Maeda S, Mizoguchi M, Ohki A, Takeshita T. 1990. Bioaccumulation of zinc and cadmium in freshwater alga, *Chlorella vulgaris*. Part I. Toxicity and accumulation. *Chemosphere* 21:953–963.
37. Sunda WG, Huntsman SA. 1996. Antagonisms between cadmium and zinc toxicity and manganese limitation in a coastal diatom. *Limnol Oceanogr* 41:373–387.
38. Tao S, Liang T, Cao J, Dawson RW, Liu CF. 1999. Synergistic effect of copper and lead uptake by fish. *Ecotoxicol Environ Saf* 44:190–195.
39. Lindon FC, Henriques FS. 1993. Effects of copper toxicity on growth and the uptake and translocation of metals in rice plants. *J Plant Nutr* 16:1449–1464.
40. Avery SV, Howlett NG, Radice S. 1996. Copper toxicity towards *Saccharomyces cerevisiae*: Dependence on plasma membrane fatty acid composition. *Appl Environ Microbiol* 62:3960–3966.
41. Hinz H. 1983. Thermodynamics of protein–ligand interactions—Calorimetric approaches. *Annu Rev Biophys Bioeng* 12:285–317.
42. Klotz IM. 1985. Ligand–receptor interactions: Facts and fantasies. *Q Rev Biophys* 18:227–259.
43. Errecalde O, Seidl M, Campbell PGC. 1998. Influence of a low molecular weight metabolite (citrate) on the toxicity of cadmium and zinc to the unicellular green algae *Selenastrum capricornutum*: An exception to the free ion activity model. *Water Res* 32:419–429.
44. Phinney JT, Bruland KW. 1994. Uptake of lipophilic organic Cu, Cd and Pb complexes in the coastal diatom *Thalassiosira weissflogii*. *Environ Sci Technol* 28:1781–1790.
45. Campbell PGC, Twiss MR, Wilkinson KJ. 1997. Accumulation of natural organic matter on the surfaces of living cells and its implication for the interaction of biota with toxic solutes. *Can J Fish Aquat Sci* 54:2543–2554.
46. Slaveykova VI, Wilkinson KJ, Ceresa A, Pretsch E. 2003. Role of fulvic acid on lead bioaccumulation to *Chlorella kesslerii*. *Environ Sci Technol* 37:1114–1121.
47. Tran D, Boudou A, Massabuau JC. 2001. How water oxygenation level influences cadmium accumulation pattern in the Asiatic clam *Corbicula fluminea*: A laboratory and field study. *Environ Toxicol Chem* 20:2073–2080.